present study is a very powerful tool to identify real target genes in each cell line. Our data revealed that MMP-13 was the most downregulated protein by miR-143 in these target genes.

MMP-13 is a proteolytic enzyme that belongs to a large family of extracellular matrix-degrading endopeptidases that are characterized by a zinc-binding motif at their catalytic sites, and the overexpression of MMP-13 has been documented in squamous cell carcinoma of head and neck,[42] lung,[43] malignant melanoma,[44] and colorectal[45] cancer. The expression in these human cancers was associated with cell cancer progression, including invasion and metastasis, diagnosis or poor outcome. In the present study, immunohistochemical analyses using clinical samples revealed that three cases expressing higher miR-143 showed few positive cells of MMP-13 in the primary lesion and all three cases were in the non-metastatic group. On the other hand, MMP-13-positive sarcoma cells were strongly or moderately observed in all lung metastasis-positive cases. These data suggested that downregulation of miR-143 led to upregulation of MMP-13 expression in human osteosarcoma cells and contributed to facilitation of lung metastasis from the primary lesion; therefore, delivering miR-143 mimic into tumor cells could prevent lung metastasis of human osteosarcoma by suppressing at least MMP-13 expression. Because a single miRNA can potentially target many mRNAs, not only MMP-13 but also the other candidate genes identified, as shown in **Supplementary Table S2**, might be involved in metastatic regulation directly or indirectly in 143B cells. Thus, it is possible that interaction of these gene products resulted in positive regulation of cell migration and/or invasion of osteosarcoma cells, and such a mechanism might be negatively regulated by miR-143 as a whole.

In conclusion, we have identified miR-143 as a metastasis-suppressive miRNA of human osteosarcoma cells and demonstrated that systemic administration of miR-143 with atelocollagen into cancer model mice was able to suppress spontaneous lung metastasis of osteosarcoma. To our knowledge, our results present the first evidence that systemic injection of miRNA/atelocollagen complexes may have therapeutic potential for the prevention of lung metastasis from osteosarcoma, although further extensive studies will be required to demonstrate the long-term efficacy and safety of nucleic acid treatment in various *in vivo* experiments. Finally, we successfully identified *MMP-13* and several other genes as probable candidates of miR-143 using a comprehensive collection system to detect miRNA-target mRNA. This system would be a powerful tool to identify single miRNA-target mRNA in a cell- or tissue-specific manner, and might contribute to reveal the mechanism of cancer generation and progression in the point of miRNA functions.

MATERIALS AND METHODS

Cell lines. Two human osteosarcoma cell lines (HOS and 143B) were obtained from the American Type Culture Collection and maintained in Dulbecco's modified Eagle's medium containing 10% heat-inactivated fetal bovine serum. The 143B cell line was generated via Kirsten mouse sarcoma virus (Ki-ras$^+$) transformation of the HOS cell line. The 143B cells were transfected with a complex of pLuc-Neo plasmid DNA (Clontech, Palo Alto, CA) and DharmaFECT (GE Healthcare, Little Chalfont, UK) in accordance with the manufacturers' instructions. Stable transfectants were selected in geneticin (600 μg/ml; Invitrogen, Carlsbad, CA). Clones expressing the luciferase gene were named *143B-Luc*.

Clinical sample. Twenty-two biopsy samples of human osteosarcomas, which did not have metastasis in the lung and other organs at first diagnosis, were obtained from the National Cancer Center Hospital. All the materials were obtained with written informed consent, and the procedures were approved by the institutional review board.

RNA extraction and quantitative real-time PCR of miRNAs. Total RNA was extracted from cell lines and clinical samples using the mirVana miRNA Isolation Kit (Ambion, Austin, TX) according to the manufacturer's protocol.

miR-143-specific complementary DNA was generated from 20 ng total RNA using the TaqMan MicroRNA RT kit (Applied Biosystems, Foster City, CA) and the miR-143-specific RT-primer from the TaqMan Micro RNA Assay (Applied Biosystems). miR-143 levels were also measured using the miR-143-specific probe included with the TaqMan Micro RNA Assay on a Real-Time PCR System 7300 and SDS software (Applied Biosystems).

miRNA microarray analysis. miRNA microarrays were manufactured by Agilent Technologies (Santa Clara, CA), and contain 470 human miRNAs [Agilent Technologies (http://www.chem.agilent.com/scripts/PHome.asp)]. Four independently extracted RNA samples were used for array analyses in each cell line. Labeling and hybridization of total RNA samples were performed according to the manufacturer's protocol. Microarray results were extracted using Agilent Feature Extraction software (v9.5.3.1) and analyzed using Gene- Spring GX 7.3.1 software (Agilent Technologies).

Transfection with synthetic miRNA and assays of cell proliferation and invasion. Synthetic has-miRs (pre-miR-hsa-miR-143, -145, -193b, -28, -149, -99b, -133, -140, -335 and negative control 1 (NC1; Ambion) or hsa-anti-miRs (Anti-miR-hsa-miR-584, -146, -31, -100, -125b, -222, -221, -29b, -625 and negative control; Ambion) were transfected into 143B-Luc cells at 30 nmol/l each (final concentration) per 1×10^6 cells/well of a 6-well plate using DharmaFECT (GE Healthcare). After 48 hours of incubation, cells were harvested and reseeded into a 96-well plate. Pre-miR- or anti-miR-transfected cells were plated at 1×10^4 cells/well in a 96-well plate and incubated for 4 days for the cell proliferation assay. The cell invasion assay was performed using CytoSelect 96-Well Cell Invasion Assay (Cell Biolabs, San Diego, CA). Pre-miR- or anti-miR-transfected cells were plated at 1×10^5 cells/well in 96-well chambers. The protocol followed the manufacturer's instructions (Cell Biolabs). Bioluminescence from 143B-Luc cells highly correlated to the total number of cells.[46] For monitoring the inhibition of cell proliferation or invasion, the cells were lysed ($n = 3$) and then analyzed for luciferase activity (Bright-Glo Luciferase Assay System; Promega, Madison, WI). Inhibition of luciferase production was normalized to the level of negative control Pre-miR- or anti-miR-transfected cells.

Animal model. Animal experiments in the present study were performed in compliance with the guidelines of the Institute for Laboratory Animal Research, National Cancer Center Research Institute. Five- to six-week-old male athymic nude mice (CLEA Japan, Shizuoka, Japan) were anesthetized by exposure to 3% isoflurane on day 0 and subsequent days. On day 0 of the experiments, to generate an experimental model, the anesthetized animals were injected with 1.5×10^6 143B-Luc cells into the right knee.[47,48]

Preparation of complex with miR-143 and atelocollagen. To prepare complexes of miRNA and atelocollagen (Koken, Tokyo, Japan), equal volumes of atelocollagen (0.1% in phosphate-buffered saline at pH 7.4) and miRNA solution were combined and mixed by rotating for 1 hour at 4 °C. The final concentration of atelocollagen was 0.05%.

Evaluation of miR-143/atelocollagen administration into spontaneous lung metastasis of osteosarcoma model mouse. One day after the 143B-Luc cell injection as above, individual mice were injected with 200 μl atelocollagen containing 50 μg miR-143 or miR-NC1 via the tail vain. miRNA/

atelocollagen complexes were injected on days 1, 4, 7, 10, 13, 16, 19, 22, and 25 postinoculation of 143B-Luc cells. Each experimental condition included 10 animals/group. For *in vivo* imaging, the mice were injected with D-luciferin (150 mg/kg; Promega) by intraperitoneal injection. Ten minutes later, photons from firefly luciferase were counted using the IVIS imaging system (Xenogen, Alameda, CA) according to the manufacturer's instructions. Data were analyzed using LivingImage software (version 2.50; Xenogen). The development of subsequent lung metastasis was monitored once a week *in vivo* by bioluminescent imaging for 4 weeks. At the end of the experiment on day 28, the primary tumor and lung of each animal were resected at necropsy for histological analysis.

Comprehensive collection and identification of miR-143 target mRNAs in 143B cells. We used two experimental approaches, immunoprecipitation of RNA-induced silencing complex by anti-Ago2 antibody (Ago2 IP) and the labeled miRNA pull-down (LAMP) assay system, to collect comprehensive target genes of miR-143. In the former method, after transfection of miR-143 or miR-NC1 into 143B, RNA-induced silencing complex was immunoprecipitated by the miRNA isolation kit, human Ago2 (Wako, Osaka, Japan) and RNA was isolated by mirVana (Ambion). The latter method, the LAMP assay system, was performed according to a previous report.[49] Briefly, cell lysate was prepared by an ultrasonic processor (Sonifier 250; Sonifier, Branson, CT) at duty cycle: 20% and output control: 1 with an interval of 30 seconds for 10 times on ice from 5 to 10×10^6 143B cells. After sonication, cell lysate was centrifuged at 15,600*g* for 30 minutes at 4 °C, and the clear cell extract was collected. Next, the pre-miR-143 sequence was amplified by PCR and then subcloned into the pSPT19 (Roche Diagnostics K.K., Tokyo, Japan). Digoxigenin-labeled pre-miR-143 or pre-miR-NC1 was transcribed by the digoxigenin RNA labeling kit (Roche), and then mixed with cell extracts. Next, this digoxigenin-labeled miRNA processed by Dicer *in vitro* was attached to its target genes by endogenous RNA-induced silencing complex. The mixtures of miRNA-target mRNA were then pulled down by anti-digoxigenin monoclonal antibody (1.71.256; Roche) and RNA was isolated by mirVana (Ambion). Finally, the isolated mRNA was reverse-transcribed to complementary DNA and 3D-Gene Human Oligo chip 25k (Toray Industries, Tokyo, Japan) was used to analyze and identify the target genes of miR-143. Genes with miR-143/miR-NC1 normalized ratios >1.1 were defined as candidates for miR-143 target genes.

Immunohistochemistry. All tumors resected from mouse primary tumors at the right knee joint were fixed with 10% buffered formalin and embedded in paraffin. Sections 3-μm thick were examined using immunohistochemistry. The sections were deparaffinized, and antigens were retrieved by autoclave in 10 mmol/l citrate buffer (pH 6.0) at 121 °C for 10 minutes. Endogenous peroxidase activity was blocked by immersing the slides in 0.6% hydrogen peroxide in methanol for 30 min. The sections were immunostained using a Histofine mouse stain kit (Nichirei, Tokyo, Japan). The primary antibodies used in this study were a mouse monoclonal antibody against human proliferative cell nuclear antigen (1:200; DAKO, Glostrup, Denmark) and a rabbit polyclonal antibody against human MMP-13 antigen (1:2,000; Abcam, Cambridge, UK). Immunoreactions were visualized with diaminobenzidine and the sections were counterstained with hematoxylin.

Western blotting. Western blotting was performed as described previously.[50] The membranes were blotted with a rabbit polyclonal antibody against human MMP-13 antigen (1:2,000; Abcam), or with a monoclonal antibody against β-actin (1:2,000; AC-15; Sigma, St Louis, MO). Signals were visualized with an enhanced chemiluminescence system (ECL Detection System; Amersham Pharmacia Biotech).

Statistical analyses. Statistical analyses were conducted using Student's *t*-test for *in vitro* screening of cell invasion and proliferation, and also to evaluate lung metastasis in an *in vivo* assay, and Welch's *t*-test was used for miR-143 expression analysis using clinical samples. $P < 0.05$ was considered significant.

SUPPLEMENTARY MATERIAL

Figure S1. Expression level of miR-143 in human osteosarcoma cell lines, 143B and HOS.
Figure S2. Effect of miRNA transfection for cell proliferation.
Figure S3. Spontaneous lung metastasis of osteosarcoma mouse model.
Figure S4. miR-143 does not effect to tumor growth in *in vivo*.
Figure S5. Six miR-143 candidate protein expression were down-regulated by miR-143 transfection in 143B.
Figure S6. No effect to expression of KRAS and ERK5 protein by miR-143 in 143B.
Table S1. Seventy-eight genes commonly detected by Ago2 IP and LAMP.
Table S2. Six candidates of miR-143 target genes.

ACKNOWLEDGMENTS

We thank Ms Ayako Inoue and Ms Ayano Matsumoto for their excellent technical assistance. The authors thank KOKEN for providing atelocollagen. This work was supported in-part by a Grant-in-Aid for the Third-Term Comprehensive 10-Year Strategy for Cancer Control, a Grant-in-Aid for Scientific Research on Priority Areas Cancer and Grant-in-Aid for Young Scientists (B) (21791395) in the Ministry of Education, Culture, Sports, Science and Technology, and the Program for Promotion of Fundamental Studies in Health Sciences of the National Institute of Biomedical Innovation (NiBio), and a Takeda Science Foundation.

REFERENCES

1. Link, MP (1993). Osteosarcoma in adolescents and young adults: new developments and controversies. Commentary on the use of presurgical chemotherapy. *Cancer Treat Res* **62**: 383–385.
2. Dorfman, HD and Czerniak, B (1995). Bone cancers. *Cancer* **75**(1 Suppl): 203–210.
3. Provisor, AJ, Ettinger, LJ, Nachman, JB, Krailo, MD, Makley, JT, Yunis, EJ *et al.* (1997). Treatment of nonmetastatic osteosarcoma of the extremity with preoperative and postoperative chemotherapy: a report from the Children's Cancer Group. *J Clin Oncol* **15**: 76–84.
4. Bacci, G, Ferrari, S, Bertoni, F, Ruggieri, P, Picci, P, Longhi, A *et al.* (2000). Long-term outcome for patients with nonmetastatic osteosarcoma of the extremity treated at the istituto ortopedico rizzoli according to the istituto ortopedico rizzoli/osteosarcoma-2 protocol: an updated report. *J Clin Oncol* **18**: 4016–4027.
5. Rytting, M, Pearson, P, Raymond, AK, Ayala, A, Murray, J, Yasko, AW *et al.* (2000). Osteosarcoma in preadolescent patients. *Clin Orthop Relat Res* : 39–50.
6. Ferguson, WS and Goorin, AM (2001). Current treatment of osteosarcoma. *Cancer Invest* **19**: 292–315.
7. Pasquinelli, AE, Reinhart, BJ, Slack, F, Martindale, MQ, Kuroda, MI, Maller, B *et al.* (2000). Conservation of the sequence and temporal expression of let-7 heterochronic regulatory RNA. *Nature* **408**: 86–89.
8. Bartel, DP (2004). MicroRNAs: genomics, biogenesis, mechanism, and function. *Cell* **116**: 281–297.
9. Lewis, BP, Burge, CB and Bartel, DP (2005). Conserved seed pairing, often flanked by adenosines, indicates that thousands of human genes are microRNA targets. *Cell* **120**: 15–20.
10. Lu, J, Getz, G, Miska, EA, Alvarez-Saavedra, E, Lamb, J, Peck, D *et al.* (2005). MicroRNA expression profiles classify human cancers. *Nature* **435**: 834–838.
11. Volinia, S, Calin, GA, Liu, CG, Ambs, S, Cimmino, A, Petrocca, F *et al.* (2006). A microRNA expression signature of human solid tumors defines cancer gene targets. *Proc Natl Acad Sci USA* **103**: 2257–2261.
12. Calin, GA, Ferracin, M, Cimmino, A, Di Leva, G, Shimizu, M, Wojcik, SE *et al.* (2005). A MicroRNA signature associated with prognosis and progression in chronic lymphocytic leukemia. *N Engl J Med* **353**: 1793–1801.
13. Jiang, J, Gusev, Y, Aderca, I, Mettler, TA, Nagorney, DM, Brackett, DJ *et al.* (2008). Association of MicroRNA expression in hepatocellular carcinomas with hepatitis infection, cirrhosis, and patient survival. *Clin Cancer Res* **14**: 419–427.
14. Cimmino, A, Calin, GA, Fabbri, M, Iorio, MV, Ferracin, M, Shimizu, M *et al.* (2005). miR-15 and miR-16 induce apoptosis by targeting BCL2. *Proc Natl Acad Sci USA* **102**: 13944–13949.
15. Meng, F, Henson, R, Wehbe-Janek, H, Ghoshal, K, Jacob, ST and Patel, T (2007). MicroRNA-21 regulates expression of the PTEN tumor suppressor gene in human hepatocellular cancer. *Gastroenterology* **133**: 647–658.
16. Asangani, IA, Rasheed, SA, Nikolova, DA, Leupold, JH, Colburn, NH, Post, S *et al.* (2008). MicroRNA-21 (miR-21) post-transcriptionally downregulates tumor suppressor Pdcd4 and stimulates invasion, intravasation and metastasis in colorectal cancer. *Oncogene* **27**: 2128–2136.
17. Osaki, M, Takeshita, F and Ochiya, T (2008). MicroRNAs as biomarkers and therapeutic drugs in human cancer. *Biomarkers* **13**: 658–670.

18. Fontana, L, Fiori, ME, Albini, S, Cifaldi, L, Giovinazzi, S, Forloni, M *et al.* (2008). Antagomir-17-5p abolishes the growth of therapy-resistant neuroblastoma through p21 and BIM. *PLoS ONE* **3**: e2236.
19. Si, ML, Zhu, S, Wu, H, Lu, Z, Wu, F and Mo, YY (2007). miR-21-mediated tumor growth. *Oncogene* **26**: 2799–2803.
20. Ma, L, Reinhardt, F, Pan, E, Soutschek, J, Bhat, B, Marcusson, EG *et al.* (2010). Therapeutic silencing of miR-10b inhibits metastasis in a mouse mammary tumor model. *Nat Biotechnol* **28**: 341–347.
21. Akao, Y, Nakagawa, Y, Kitade, Y, Kinoshita, T and Naoe, T (2007). Downregulation of microRNAs-143 and -145 in B-cell malignancies. *Cancer Sci* **98**: 1914–1920.
22. Crawford, M, Brawner, E, Batte, K, Yu, L, Hunter, MG, Otterson, GA *et al.* (2008). MicroRNA-126 inhibits invasion in non-small cell lung carcinoma cell lines. *Biochem Biophys Res Commun* **373**: 607–612.
23. Valastyan, S, Reinhardt, F, Benaich, N, Calogrias, D, Szász, AM, Wang, ZC *et al.* (2009). A pleiotropically acting microRNA, miR-31, inhibits breast cancer metastasis. *Cell* **137**: 1032–1046.
24. Tazawa, H, Tsuchiya, N, Izumiya, M and Nakagama, H (2007). Tumor-suppressive miR-34a induces senescence-like growth arrest through modulation of the E2F pathway in human colon cancer cells. *Proc Natl Acad Sci USA* **104**: 15472–15477.
25. Luu, HH, Kang, Q, Park, JK, Si, W, Luo, Q, Jiang, W *et al.* (2005). An orthotopic model of human osteosarcoma growth and spontaneous pulmonary metastasis. *Clin Exp Metastasis* **22**: 319–329.
26. Peltier, HJ and Latham, GJ (2008). Normalization of microRNA expression levels in quantitative RT-PCR assays: identification of suitable reference RNA targets in normal and cancerous human solid tissues. *RNA* **14**: 844–852.
27. Calin, GA and Croce, CM (2006). MicroRNA signatures in human cancers. *Nat Rev Cancer* **6**: 857–866.
28. Ochiya, T, Takahama, Y, Nagahara, S, Sumita, Y, Hisada, A, Itoh, H *et al.* (1999). New delivery system for plasmid DNA *in vivo* using atelocollagen as a carrier material: the Minipellet. *Nat Med* **5**: 707–710.
29. Takeshita, F, Minakuchi, Y, Nagahara, S, Honma, K, Sasaki, H, Hirai, K *et al.* (2005). Efficient delivery of small interfering RNA to bone-metastatic tumors by using atelocollagen in vivo. *Proc Natl Acad Sci USA* **102**: 12177–12182.
30. Takeshita, F, Patrawala, L, Osaki, M, Takahashi, RU, Yamamoto, Y, Kosaka, N *et al.* (2010). Systemic delivery of synthetic microRNA-16 inhibits the growth of metastatic prostate tumors via downregulation of multiple cell-cycle genes. *Mol Ther* **18**: 181–187.
31. Cho, WC (2007). OncomiRs: the discovery and progress of microRNAs in cancers. *Mol Cancer* **6**: 60.
32. Ma, L, Teruya-Feldstein, J and Weinberg, RA (2007). Tumour invasion and metastasis initiated by microRNA-10b in breast cancer. *Nature* **449**: 682–688.
33. Tavazoie, SF, Alarcón, C, Oskarsson, T, Padua, D, Wang, Q, Bos, PD *et al.* (2008). Endogenous human microRNAs that suppress breast cancer metastasis. *Nature* **451**: 147–152.
34. Suzuki, HI, Yamagata, K, Sugimoto, K, Iwamoto, T, Kato, S and Miyazono, K (2009). Modulation of microRNA processing by p53. *Nature* **460**: 529–533.
35. Kent, OA, Chivukula, RR, Mullendore, M, Wentzel, EA, Feldmann, G, Lee, KH *et al.* (2010). Repression of the miR-143/145 cluster by oncogenic Ras initiates a tumor-promoting feed-forward pathway. *Genes Dev* **24**: 2754–2759.
36. Michael, MZ, O' Connor, SM, van Holst Pellekaan, NG, Young, GP and James, RJ (2003). Reduced accumulation of specific microRNAs in colorectal neoplasia. *Mol Cancer Res* **1**: 882–891.
37. Porkka, KP, Pfeiffer, MJ, Waltering, KK, Vessella, RL, Tammela, TL and Visakorpi, T (2007). MicroRNA expression profiling in prostate cancer. *Cancer Res* **67**: 6130–6135.
38. Lui, WO, Pourmand, N, Patterson, BK and Fire, A (2007). Patterns of known and novel small RNAs in human cervical cancer. *Cancer Res* **67**: 6031–6043.
39. Iorio, MV, Visone, R, Di Leva, G, Donati, V, Petrocca, F, Casalini, P *et al.* (2007). MicroRNA signatures in human ovarian cancer. *Cancer Res* **67**: 8699–8707.
40. Chen, X, Guo, X, Zhang, H, Xiang, Y, Chen, J, Yin, Y *et al.* (2009). Role of miR-143 targeting KRAS in colorectal tumorigenesis. *Oncogene* **28**: 1385–1392.
41. Tome, Y, Tsuchiya, H, Hayashi, K, Yamauchi, K, Sugimoto, N, Kanaya, F *et al.* (2009). *In vivo* gene transfer between interacting human osteosarcoma cell lines is associated with acquisition of enhanced metastatic potential. *J Cell Biochem* **108**: 362–367.
42. Stokes, A, Joutsa, J, Ala-Aho, R, Pitchers, M, Pennington, CJ, Martin, C *et al.* (2010). Expression profiles and clinical correlations of degradome components in the tumor microenvironment of head and neck squamous cell carcinoma. *Clin Cancer Res* **16**: 2022–2035.
43. Hsu, CP, Shen, GH and Ko, JL (2006). Matrix metalloproteinase-13 expression is associated with bone marrow microinvolvement and prognosis in non-small cell lung cancer. *Lung Cancer* **52**: 349–357.
44. Corte, MD, Gonzalez, LO, Corte, MG, Quintela, I, Pidal, I, Bongera, M *et al.* (2005). Collagenase-3 (MMP-13) expression in cutaneous malignant melanoma. *Int J Biol Markers* **20**: 242–248.
45. Huang, MY, Chang, HJ, Chung, FY, Yang, MJ, Yang, YH, Wang, JY *et al.* (2010). MMP13 is a potential prognostic marker for colorectal cancer. *Oncol Rep* **24**: 1241–1247.
46. Jenkins, DE, Oei, Y, Hornig, YS, Yu, SF, Dusich, J, Purchio, T *et al.* (2003). Bioluminescent imaging (BLI) to improve and refine traditional murine models of tumor growth and metastasis. *Clin Exp Metastasis* **20**: 733–744.
47. Berlin, O, Samid, D, Donthineni-Rao, R, Akeson, W, Amiel, D and Woods, VL Jr (1993). Development of a novel spontaneous metastasis model of human osteosarcoma transplanted orthotopically into bone of athymic mice. *Cancer Res* **53**: 4890–4895.
48. Miretti, S, Roato, I, Taulli, R, Ponzetto, C, Cilli, M, Olivero, M *et al.* (2008). A mouse model of pulmonary metastasis from spontaneous osteosarcoma monitored *in vivo* by Luciferase imaging. *PLoS ONE* **3**: e1828.
49. Hsu, RJ, Yang, HJ and Tsai, HJ (2009). Labeled microRNA pull-down assay system: an experimental approach for high-throughput identification of microRNA-target mRNAs. *Nucleic Acids Res* **37**: e77.
50. Hayashi, H, Tatebe, S, Osaki, M, Goto, A, Sato, K and Ito, H (1998). Anti-Fas antibody-induced apoptosis in human colorectal carcinoma cell lines: role of the p53 gene. *Apoptosis* **3**: 431–437.

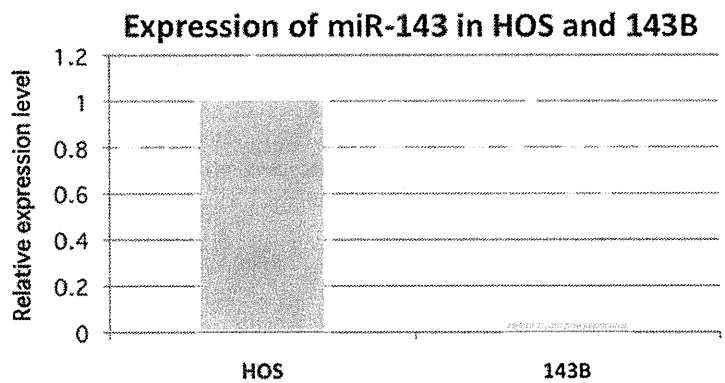
Expression of miR-143 in HOS and 143B
Relative expression level
1.2
1
0.8
0.6
0.4
0.2
0
HOS
143B

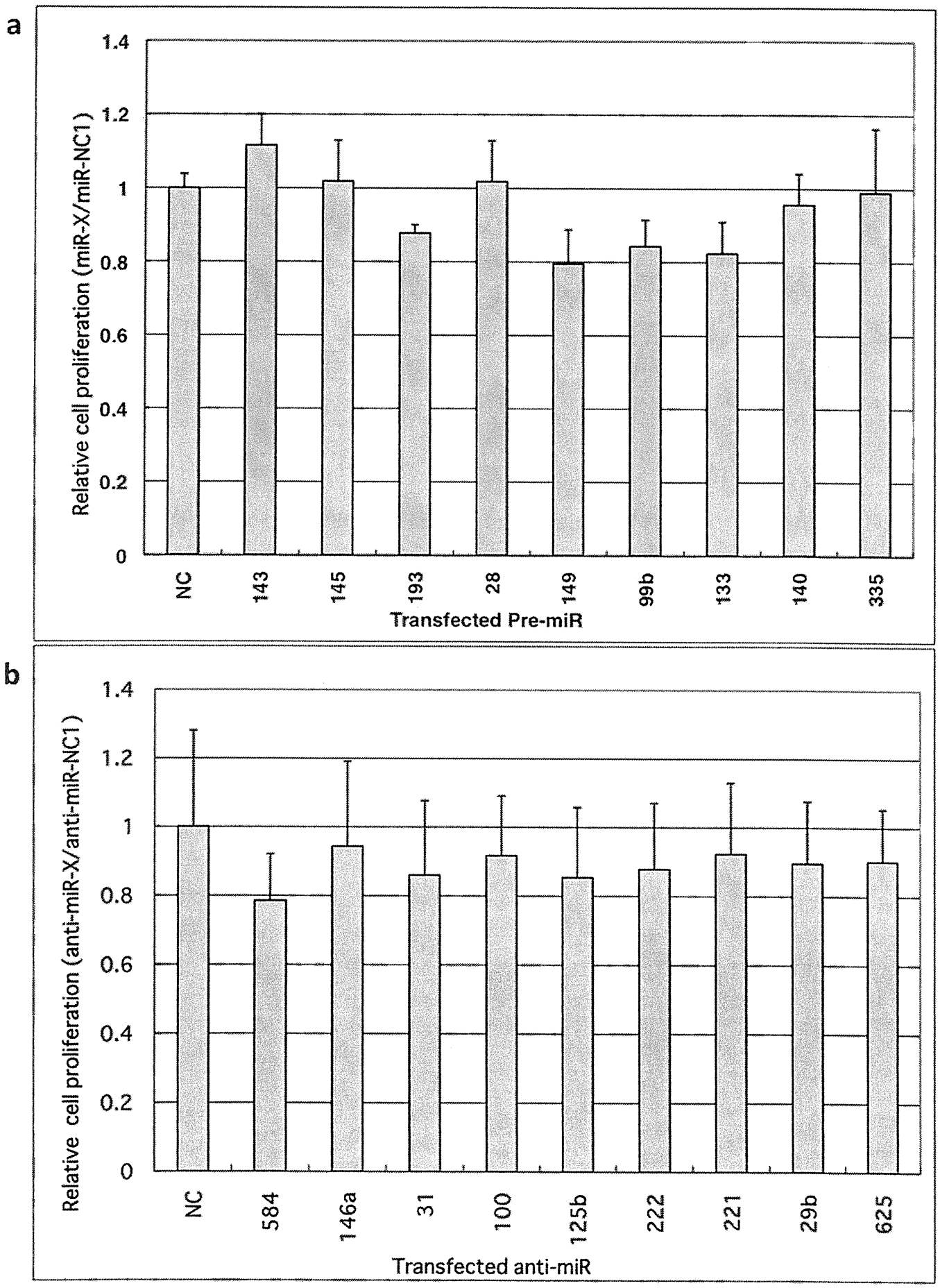
a
1.4
1.2
1
0.8
0.6
0.4
0.2
0
Relative cell proliferation (miR-X/miR-NC1)
NC
143
145
193
28
149
99b
133
140
335
Transfected Pre-miR
b
1.4
1.2
1
0.8
0.6
0.4
0.2
0
Relative cell proliferation (anti-miR-X/anti-miR-NC1)
NC
584
146a
31
100
125b
222
221
29b
625
Transfected anti-miR

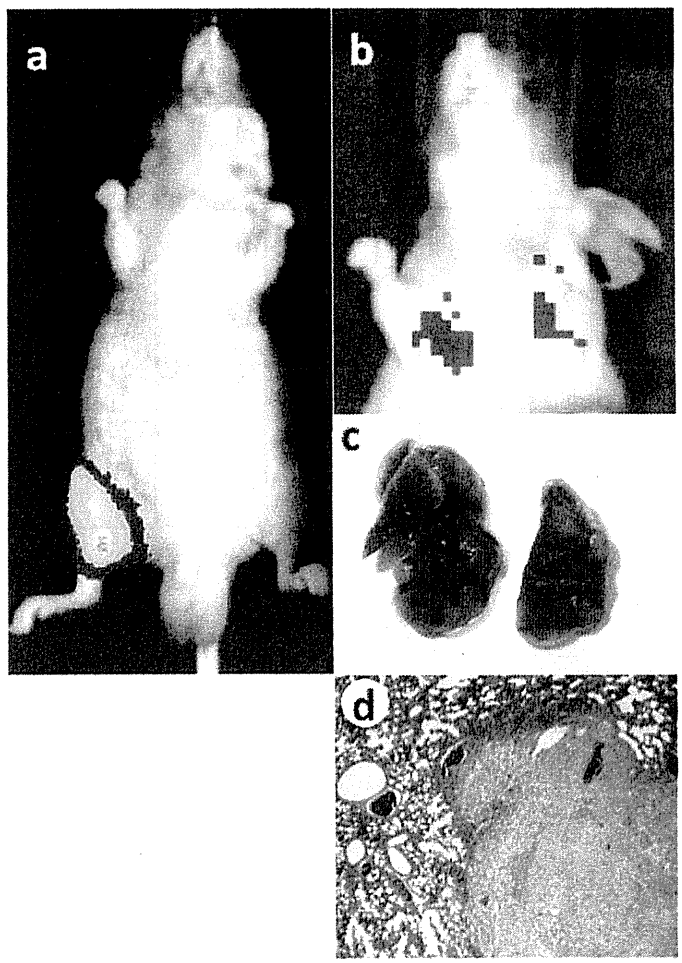
a
b
c
d

miR-143 / 0.05%Atelocollagen

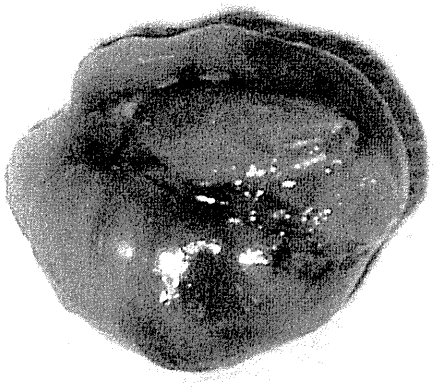

3.32 ± 0.65g

Primary tumor

3.67 ± 0.59g

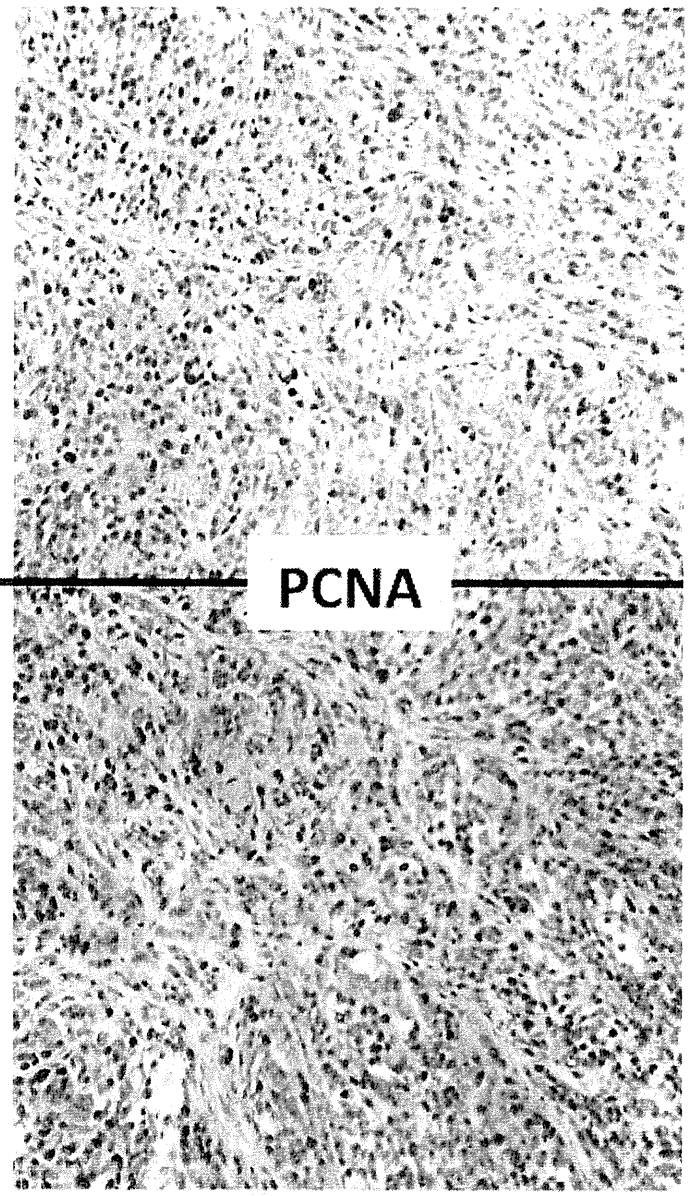

miR-NC1 / 0.05%Atelocollagen

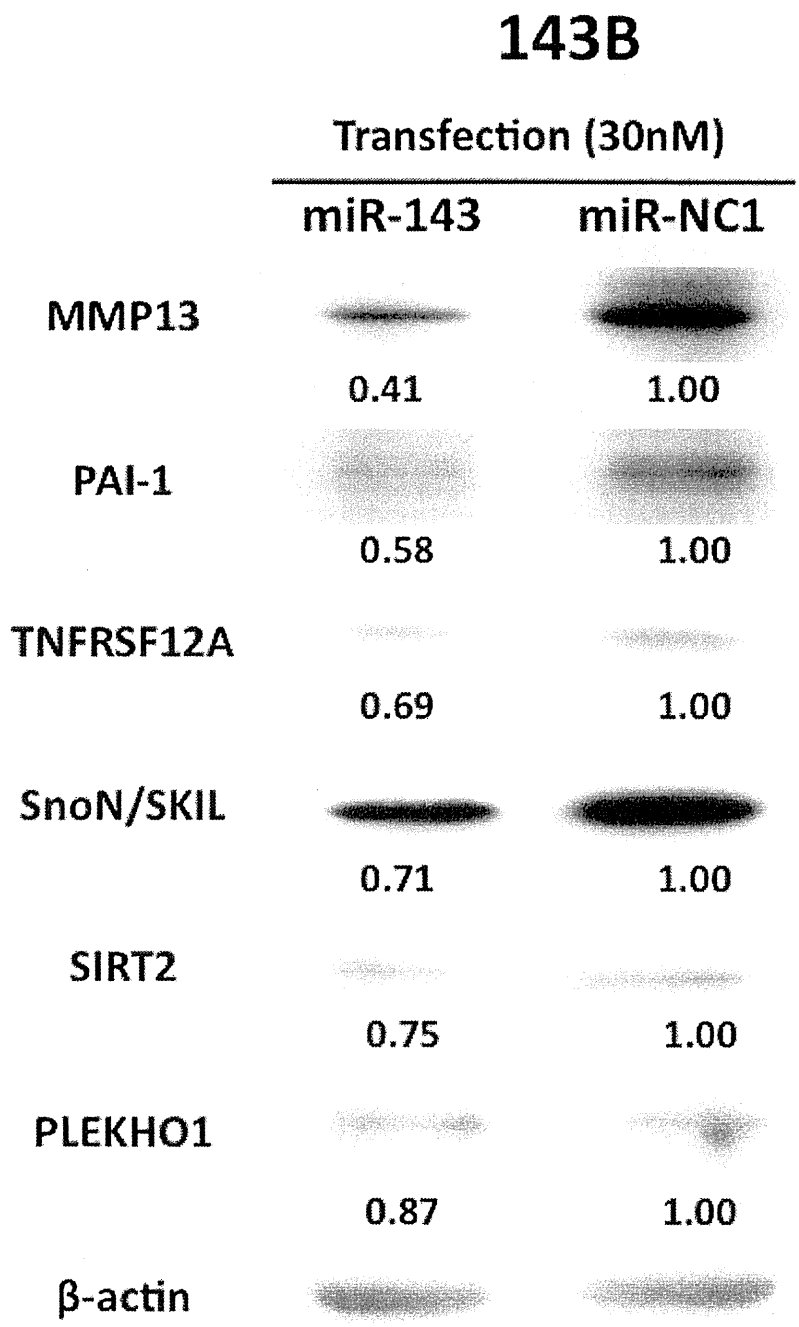
143B
Transfection (30nM)
miR-143
miR-NC1
MMP13
0.41
1.00
PAI-1
0.58
1.00
TNFRSF12A
0.69
1.00
SnoN/SKIL
0.71
1.00
SIRT2
0.75
1.00
PLEKHO1
0.87
1.00
β-actin

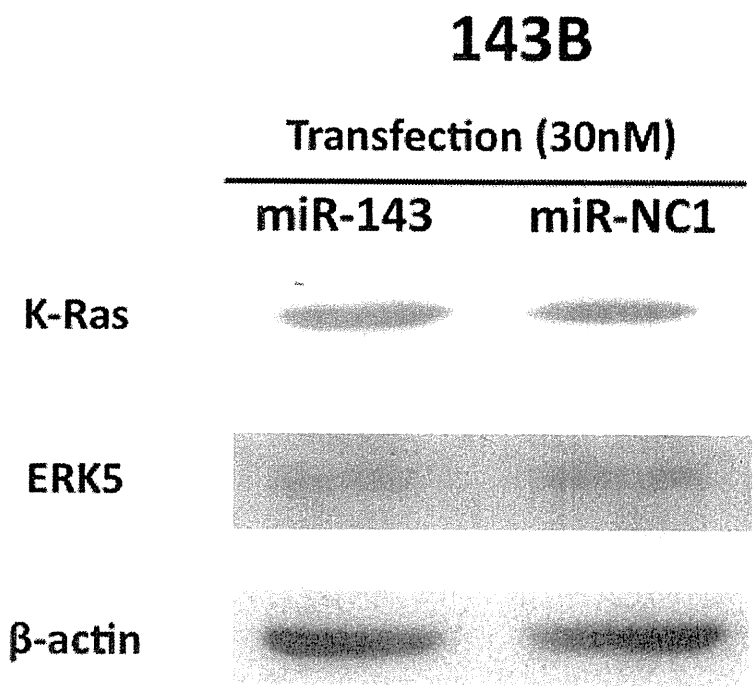
143B
Transfection (30nM)
miR-143
miR-NC1
K-Ras
ERK5
β-actin

Table S1 Seventy-eight genes commonly detected by Ago2 IP & LAMP

AKAP8L	IQCA	Q8IZ67_HUMAN
ANGPTL4	JMJD2B	Q96G28_HUMAN
ANKRD11	KLF12	RALGDS
ANXA6	LGP2_HUMAN	RANGAP1
ARID4A	LIN7A	RBM27
ARL7	LRRC14	RGS3
ATAD3B	MAG	RHEBL1
BAX	MMP13	RNPEPL1
BSCL2	MORF4	SERPINE1
C10_HUMAN	MXD4	SIRT2_HUMAN
CAN12_HUMAN	NOLA1	SKIL
CDKN2B	NP_004806.2	SOX4
CENTG3	NP_055495.2	STX16
COL6A2	NP_115726.1	TAF6L
COL7A1	NP_612398.1	TCP10L
ELA3A	NP_777610.1	TNFAIP8
ENST00000281815	NP_848130.1	TNFRSF12A
EPIM	NP_940865.1	TNIP2
FARP2	NP_997215.1	TP53INP1
G1P2	NUP160	TRIM65
GPC1	PFKFB4	TTLL3
GPR123	PICALM	U222_HUMAN
GRB2_HUMAN	PPFIA3	WAC
HECTD2	PTPN12	XP_032996.2
HECW2	Q5T7L7_HUMAN	ZFP276
HES4	Q8IZ51_HUMAN	ZFP36

Table S2 Six candidates of miR-143 target genes

SERPINE1/PAI-1
PLEKHO1
SIRT2
SKIL/SnoN
MMP13
TNFRSF12A

iPS細胞のエピゲノム

――再生医療に向けたiPS細胞のクオリティコントロールにおけるエピゲノム解析の有用性

Epigenetics in iPS cells

山田泰広(写真)　山中伸弥

Yasuhiro YAMADA[1,2] and Shinya YAMANAKA[1]

京都大学 iPS 細胞研究所[1]，科学技術振興機構さきがけ[2]

◎iPS 細胞(induced pluripotent stem cell)はすべての体細胞に分化しうるという点で，再生医療のソースとして大きな期待を集めている．しかし，樹立された iPS 細胞の性質にはライン間でのバリエーションが存在することが明らかとなり，再生医療の実現のために，均一で質の高い iPS 細胞の作製や，iPS 細胞の個性に準じた応用方法の開発が望まれている．近年，エピジェネティック修飾状態の差異が iPS 細胞の質に変化を及ぼしうることが明らかとなりつつある．再生医療に有用な iPS 細胞の樹立・選別のためには，iPS 細胞におけるエピゲノム解析およびエピゲノム制御機構の理解が非常に重要な課題となると考えられる．本稿では iPS 細胞のエピゲノム制御について最新の知見を紹介し，それらの知見を背景とした iPS 細胞の再生医療に向けた応用の可能性について議論したい．

Key word：iPS細胞，再生医療，疾患特異的 iPS 細胞

分化した体細胞に 4 つの異なる転写因子を導入することで，胚性幹細胞(ES 細胞)とほぼ同等の細胞，すなわち induced pluripotent stem cell(iPS 細胞)の樹立が可能となった[1,2]．iPS 細胞樹立の過程はエピジェネティック修飾状態の大きな改変を伴い，エピゲノムのリセットが重要な役割を果たすことが明らかとなりつつある．iPS 細胞はすべての体細胞に分化しうるという点で，再生医療のソースとして大きな期待を集めている．しかし一方で，樹立された iPS 細胞の性質には細胞株間でのバリエーションが存在することが明らかとなり，再生医療の実現のために，均一で質の高い iPS 細胞の作製や，iPS 細胞の個性に準じた応用方法の開発が望まれている．iPS 細胞のクオリティや個性はエピジェネティック修飾状態の差異に由来する可能性が考えられ，再生医療に有用な iPS 細胞の樹立・選別のためには，iPS 細胞におけるエピゲノム解析およびエピゲノム制御機構の理解が重要な課題となるであろう．

本稿では ES 細胞，iPS 細胞をはじめとする多能性幹細胞のエピゲノム制御について最新の知見を紹介し，それらの知見を背景とした iPS 細胞の再

サイドメモ　疾患特異的iPS細胞

多くの疾患において，疾患発症に関与する遺伝子の配列異常や SNP の違いが報告されている．遺伝的背景が発症に関与した疾患において iPS 細胞(疾患特異的 iPS 細胞)を樹立することで，病態解明や治療法開発をめざす試みがなされている．さまざまな疾患特異的 iPS 細胞を作製し，それぞれの疾患において原因となる機能性体細胞へ分化誘導させることで，疾患のモデル細胞を作製しようとする研究が盛んに行われている．iPS 細胞は患者自身の体細胞から樹立でき，疾患原因細胞への分化誘導が可能であるのみならず，無限に細胞供給できることは，疾患特異的 iPS 細胞を用いた研究において大きな利点となりうる．このように，iPS 細胞は再生医療のソースとしての応用が注目されているのみならず，病態解明や新規治療方法の開発におけるツールとしても大きな期待が寄せられている．

生医療への応用の可能性について議論したい.

ES細胞のエピゲノム

ES 細胞(embryonic stem cell)は胚盤胞の内部細胞塊から樹立される細胞で,個体すべての細胞に分化しうる多能性を有している一方で,無限の細胞増殖能をもちあわせている.ES 細胞の DNA 一次配列は基本的に分化細胞と同一であることから,ES 細胞の多能性維持,分化の制御には転写因子による制御と密接に関連したエピゲノムのコントロールが重要な役割を果たしていることが予想される.ES 細胞の多能性維持には,Oct3/4, Nanog, Sox2 の転写因子によるコアネットワークの活性化が必須であることが示され,転写因子の重要性が強調されてきた[3].

一方で,DNA メチル化やヒストン修飾などのエピジェネティック修飾状態変化を誘導するエピゲノム制御がどのようにして ES 細胞の多能性を維持しているのか,一方で複数の細胞系譜への分化を許容するフレキシブルな状態を維持しているのかについては,いまだ不明な点が多い.次世代高速シークエンサーをはじめとする解析技術の進歩により,ES 細胞におけるゲノム網羅的なエピゲノム解析が行われ,多能性細胞に特徴的ないくつかのエピジェネティック修飾状態およびエピゲノム制御機構が明らかになりつつある.

DNAメチル化

シトシンのメチル化は遺伝子発現制御,個体発生,各種疾患に重要な役割を果たすことが示されており,エピゲノム制御の中心的存在のひとつとなっている[4].DNA のメチル化はサイレントなクロマチン状態と相関があり,一般にプロモーター領域の DNA メチル化はその遺伝子発現量とは負の相関がみられる.メチル化シトシンに対する抗体,メチル化 DNA 結合ドメイン(MBD)やメチル化感受性制限酵素などと次世代高速シークエンサーを組み合わせた方法により,ES 細胞におけるゲノムスケールでの DNA メチル化マップが作成された.

以前から哺乳類シトシンのメチル化は CpG 配列のシトシンに存在すると考えられてきた.しかし,ヒト ES 細胞においては約 1/4 のメチル化シトシンは非 CpG 配列(CNG および CNN)にみられることが最近報告された[5].ヒト分化細胞ではほぼすべてのメチル化シトシンが CpG 配列に検出されることから,非 CpG 配列のシトシンメチル化は ES 細胞特異的な現象と考えられ,機能的な意義解明が待たれる.

ヒストン修飾およびヒストンバリアント

ヒストンの 60 種類以上の残基にメチル化,アセチル化,リン酸化などによるさまざまな化学的修飾が観察される.DNA メチル化マップと同様にして,修飾ヒストンに対する抗体により濃縮されたヌクレオソームからの DNA 断片を次世代シークエンサーで同定することによりゲノムスケールでのヒストン修飾パターンが明らかとなってきた.転写活性化領域にはヒストン H4 のアセチル化,H3 の 4 番目のリジン(H3K4)のメチル化がしばしば観察され,反対に転写不活性化領域には H3K9 メチル化,H3K27 のメチル化が濃縮されている.ES 細胞においては,細胞分化に重要な遺伝子は転写活性化マークの H3K4 メチル化と不活性化マークである H3K27 メチル化が同時に存在する"bivalent domain"を形成し,転写が抑制されている[6].ES 細胞の分化により bivalent domain における H3K27 メチル化が解除されることにより,H3K4 メチル化単独の univalent domain へと変化するとともに,速やかに転写が活性化される.DNA 脱メチル化酵素の有無についての議論がはじまって久しいが,DNA メチル化は安定したエピジェネティック修飾であることを考えると,ES 細胞/iPS 細胞における遺伝子発現制御のフレキシビリティーとして bivalent domain をはじめとするヒストン修飾状態が重要な役割を果たしていることが想像される.

ヒストンの修飾に加えてヒストンそのものにおけるバリアントの存在が知られる.そのなかでも H2AZ は ES 細胞において転写不活性化因子であるポリコーム群複合体の標的部位に濃縮されており,機能的にも転写に抑制的に働いていることが示された.未分化性維持,細胞分化の制御にはヌクレオソームにおけるヒストンバリアントの使い

分けも関与していることが明らかとなりつつある[7].

多能性幹細胞分化に伴うエピゲノムの変化

細胞分化に伴い，エピゲノムが変化することが予想されてきたものの，具体的な変化に関しての情報はいまだ乏しい．Meissner らは ES 細胞と神経幹細胞の DNA メチル化状態をゲノム網羅的に解析し，ヒストン修飾状態と比較検討した[8]．その結果，予想されていたように，DNA メチル化状態は細胞の分化により大きく変化することが確認された．

注目すべきは，細胞分化によって DNA メチル化状態が変化する領域は highly conserved non-coding element とよばれる領域に顕著であり，いままで注目されてきた CpG island が存在するコアプロモーター領域では大きな変化が少ないことであった．さらに，ES 細胞と神経幹細胞の DNA メチル化状態の比較により，基本的に DNA メチル化レベルは CpG 配列の密度に反比例する傾向がみられるが，その例外もしばしば観察されることが明らかになった．その反面，DNA メチル化の変化はヒストンの修飾パターンの変化と非常によく相関することが示された．この現象は DNA メチル化パターンの形成は DNA の一次配列に依存しているというよりも，エピジェネティック修飾状態自身により決定されることを示唆している．これら Meissner らの仕事のなかで，神経幹細胞由来アストロサイトを試験管内で培養し継代を繰り返すと，CpG 密度の高い領域において異常な DNA メチル化が出現しはじめることが示された．このことは培養細胞を用いたエピジェネティック修飾状態の解析に対して警鐘を鳴らすとともに，癌細胞における CpG island の異常メチル化の由来を示唆する結果と考えられ，意義深い．

iPS細胞の樹立とリプログラミングによるエピゲノムの変化

2006 年，分化したマウス体細胞に 4 つの転写因子，Oct3/4，Sox2，Klf4，Myc を導入することで，多能性をもった iPS 細胞の樹立が可能となった[2]．2007 年には，ヒト細胞においても iPS 細胞の樹立が可能となり[1]，現在再生医療への応用に向けた取組みがなされている[9,10]．iPS 細胞の樹立のメカニズムはいまだ不明な点が多い．すくなくとも，iPS 細胞の樹立には週単位の時間を必要とする一方で，4 因子が導入されても大部分の細胞はリプログラミングに失敗することが明らかになっている．より効率的なリプログラミング法開発，そして再生医療を念頭においた安全なリプログラミング法開発のためには，リプログラミング過程の詳細な理解が必要と考えられる．

iPS 細胞は ES 細胞に類似した形態，生物学的特徴を示すのみならず，iPS 細胞のエピジェネティック修飾状態は ES 細胞の修飾状態に類似していることが示された．すなわち，リプログラミング過程では分化細胞のエピジェネティック修飾パターンから ES 細胞のパターンへと大きく変化する．実際に，マウス iPS 細胞でのヒストン修飾状態は ES 細胞に類似したパターンを有し，X 染色体の再活性化も確認されているし[11]，ヒト iPS 細胞とヒト ES 細胞のヒストン修飾状態に明らかな違いがないことが報告されている．したがって，エピジェネティック修飾状態の改変がリプログラミングの重要なイベントであることが予想されている．

以前から分化細胞の核は脱核した卵子への核移植，および embryonal carcinoma 細胞(EC 細胞)/ES 細胞との細胞融合によってリプログラミングされることが示されてきた[12-14]．iPS 細胞の樹立には週単位の時間が必要であるのに対して，核移植によるリプログラミングは 1〜2 日以内に，しかもわずか 1〜2 回の細胞分裂の間に速やかに誘導され，リプログラミングに要する時間がまったく異なる．すなわち，iPS 細胞樹立と核移植はリプログラミング経路が異なることが示唆される．

この 2 つのリプログラミング過程の違いを説明しうるひとつの因子は DNA 脱メチル化反応と考えられる[15]．DNA メチル化は DNA 合成に際して，おもに DNA methyltransferase 1(DNMT1)により安定的に維持されることがわかっている．一方で，一度付加されたシトシンのメチル基がはずれる，すなわち脱メチル化反応については 2 つの異なる系が提唱されている．ひとつは受動的な脱メチル

化反応で，DNA 複製の際に，メチル基を新規合成 DNA 鎖に付加せず，結果的にメチル化レベルが低下する系である．他方は能動的脱メチル化反応である．受精直後の雄性核は速やかに DNA メチル化レベルが低下することが観察されている．このメチル化レベルの低下には新規 DNA 合成は伴っておらず，初期の受精卵には積極的に DNA メチル化を解除する機構が存在することが示唆されている．

近年，AID/Mbd4/Gadd45a による deamination, glycosylation を介した脱メチル化反応のメカニズムが提唱されている[16,17]．体細胞においては明らかな能動的 DNA 脱メチル化反応は証明されておらず，能動的脱メチル化反応は受精卵などの特殊な細胞における特異的な反応であることが示唆されている．ES 細胞との細胞融合によるリプログラミングにおいては *Nanog* locus の DNA 脱メチル化は DNA 複製を伴わず，わずか 1 日の間に観察され，iPS 細胞樹立の過程と比べると非常に短時間で DNA 脱メチル化反応が生じることから，能動的 DNA 脱メチル化反応の関与が予想されている．

一方で，体細胞に転写因子を導入する iPS 細胞樹立の過程では *Nanog* locus などの DNA 脱メチル化は late event であり，核移植，細胞融合における脱メチル化に比べて長い時間を要することが示されている．体細胞において能動的 DNA 脱メチル化反応が存在しないとすれば，能動的脱メチル化反応の有無がリプログラミングに要する時間を規定している可能性がある．実際に AID の発現を低下させた ES 細胞との細胞融合によるリプログラミングにおいて，AID が DNA 脱メチル化反応および *OCT3/4* や *NANOG* の活性化に必要であることが示され，すくなくとも細胞融合によるリプログラミングには AID を介した能動的 DNA 脱メチル化反応が関与していることが示唆されている[17]．

以上から，能動的 DNA 脱メチル化反応の積極的な誘導が可能であれば，iPS 細胞樹立過程において樹立効率の向上，スピード促進が期待されるのみならず，iPS 細胞の質の向上にもつながる可能性が考えられる．まずは能動的脱メチル化反応のメカニズム解明が重要であろう．AID/Mbd4/Gadd 45a による脱メチル化反応に加えて，Tet による水酸化メチル化シトシンへの変換を介したシトシン脱メチル化反応の可能性が提唱されている．実際に Tet は ES 細胞未分化性維持機構への関与が報告されており[18]，今後の研究の展開が期待される．

iPS細胞とES細胞とのエピゲノム比較

前述のように iPS 細胞は ES 細胞に類似した遺伝子発現パターンを示すのみならず，ヒストンの修飾パターン，DNA メチル化状態などのエピジェネティック修飾状態においても ES 細胞とほぼ同一の特徴を有している．しかし，iPS 細胞が胚盤胞内部細胞塊由来の ES 細胞と完全に同一の性質を有するかどうかについては議論が続いている．実際に，多くのマウス iPS 細胞は ES 細胞に比べてキメラマウスにおけるキメラ寄与率が低いことが知られ，tetraploid complementation assay においては，ほとんどのマウス iPS 細胞では全身が iPS 細胞に由来するマウスは作製できないことが知られてきた．最近，一部のマウス iPS 細胞においては *Dlk1-Dio3* 遺伝子インプリント領域における遺伝子発現が ES 細胞と比べて抑制されていることが報告された[19]．興味深いことに，*Dlk1-Dio3* 遺伝子領域の発現低下を伴う iPS 細胞では，*Dlk1-Dio3* 遺伝子領域の DMR(differentially methylated region)の DNA メチル化パターンの異常がみられ，iPS 細胞からのマウス形成能にも影響が観察されるという．エピジェネティック修飾状態の違いが iPS 細胞の性質を変化させうることを示唆しているかもしれない．今後，これらが普遍的に iPS 細胞全体に適応されるのかを慎重に検証する必要がある．

iPS細胞の由来による性質の違い

異なる細胞から樹立された iPS 細胞はその由来細胞へ分化しやすいことが報告された[20,21]．たとえば，血液由来の iPS 細胞は血液に分化しやすく，間葉系由来の iPS 細胞はより骨に分化しやすい性質を有する．さらには異なる細胞から樹立された iPS 細胞は，DNA メチル化修飾パターンの違いか

ら区別しうることが報告された．すなわち，iPS細胞には由来する細胞のepigenetic memoryが存在することが示唆された．Epigenetic memoryの存在を検証し理解するためには，iPS細胞の分化指向性と具体的なDNAメチル化状態の差異との関連を明らかする必要があるであろう．興味深いことに，核移植によりリプログラミングされたntES細胞のDNAメチル化状態はiPS細胞に比べて，よりES細胞に近いことが報告された．核移植によるリプログラミングがより効率的にエピジェネティック修飾状態を改変しうる可能性を示している．

上述したように，DNAメチル化はより安定的で“deep”なサイレンシングに関与していると考えられており，核移植後の卵子に存在する能動的DNA脱メチル化反応の存在が，効率的なDNAメチル化状態改変に重要な役割を果たしているのかもしれない．

再生医療に向けたiPS細胞のクオリティコントロールとエピゲノム

再生医療に使用するiPS細胞のクオリティーコントロールの観点から，iPS細胞株間での分化指向性の違いや，由来細胞に依存したiPS細胞株間のDNAメチル化修飾状態の違いはiPS細胞の質のバリエーションを示唆するものであり，均一なiPS細胞を選別するためにはエピゲノム解析が有用と考えられる．しかし，エピゲノムの違いがどのように，そしてどの程度iPS細胞の質に影響を与えるのかはいまだ不明である．

今後はiPS細胞の詳細なエピゲノム解析に加えて，細胞分化を規定するエピゲノム制御機構の理解を深めることが重要と考えられる．エピジェネティック修飾状態はDNA脱メチル化剤やヒストン脱アセチル化酵素阻害剤などの処理により変化させうることが示唆されており，エピジェネティック修飾薬剤の利用および新規開発は質の高い均一なiPS細胞を得るためのアプローチとなりうるであろう．iPS細胞は再生医療への応用において期待されているのみならず，疾患特異的iPS細胞を用いた病態解析において非常に有用なツールとなっている．疾患特異的iPS細胞の性質を評価する場合には，iPS細胞自体におけるエピジェネティック修飾状態のばらつきの存在を念頭におき，疾患本来の表現形との明確な区別をすることが重要となるであろう．一方で，エピジェネティック修飾状態の差異はiPS細胞の個性ととらえることもできる．効率的な機能性分化細胞の誘導のために，エピジェネティック修飾状態の違いに由来するiPS細胞の個性を積極的に利用するアプローチが有効かもしれない．

文献

1) Takahashi, K. et al. : Induction of pluripotent stem cells from adult human fibroblasts by defined factors. *Cell*, **131** : 861-872, 2007.
2) Takahashi, K. and Yamanaka, S. : Induction of pluripotent stem cells from mouse embryonic and adult fibroblast cultures by defined factors. *Cell*, **126** : 663-676, 2006.
3) Niwa, H. : How is pluripotency determined and maintained? *Development*, **134** : 635-646, 2007.
4) Jaenisch, R. and Bird, A. : Epigenetic regulation of gene expression : how the genome integrates intrinsic and environmental signals. *Nat. Genet.*, **33** (Suppl.) : 245-254, 2003.
5) Lister, R. et al. : Human DNA methylomes at base resolution show widespread epigenomic differences. *Nature*, **462** : 315-322, 2009.
6) Bernstein, B. E. et al. : A bivalent chromatin structure marks key developmental genes in embryonic stem cells. *Cell*, **125** : 315-326, 2006.
7) Creyghton, M. P. et al. : H2AZ is enriched at polycomb complex target genes in ES cells and is necessary for lineage commitment. *Cell*, **135** : 649-661, 2008.
8) Meissner, A. et al. : Genome-scale DNA methylation maps of pluripotent and differentiated cells. *Nature*, **454** : 766-770, 2008.
9) Okita, K. et al. : Generation of mouse-induced pluripotent stem cells with plasmid vectors. *Nat. Protoc.*, **5** : 418-428, 2010.
10) Nakagawa, M. et al. : Promotion of direct reprogramming by transformation-deficient Myc. *Proc. Natl. Acad. Sci. USA*, **107** : 14152-14157, 2010.
11) Maherali, N. et al. : Directly reprogrammed fibroblasts show global epigenetic remodeling and widespread tissue contribution. *Cell Stem Cell*, **1** : 55-70, 2007.
12) Gurdon, J. : Nuclear reprogramming in eggs. *Nat. Med.*, **15** : 1141-1144, 2009.
13) Wilmut, I. et al. : Viable offspring derived from fetal and adult mammalian cells. *Nature*, **385** : 810-813, 1997.
14) Miller, R. A. and Ruddle, F. H. : Pluripotent teratocarcinoma-thymus somatic cell hybrids. *Cell*, **9** : 45-55, 1976.
15) Yamanaka, S. and Blau, H. M. : Nuclear reprogramming to a pluripotent state by three approaches.

Nature, **465** : 704-712, 2010.
16) Rai, K. et al. : DNA demethylation in zebrafish involves the coupling of a deaminase, a glycosylase, and gadd45. *Cell*, **135** : 1201-1212, 2008.
17) Bhutani, N. et al. : Reprogramming towards pluripotency requires AID-dependent DNA demethylation. *Nature*, **463** : 1042-1047, 2010.
18) Ito, S. et al. : Role of Tet proteins in 5mC to 5hmC conversion, ES-cell self-renewal and inner cell mass specification. *Nature*, **466** : 1129-1133, 2010.
19) Stadtfeld, M. et al. : Aberrant silencing of imprinted genes on chromosome 12qF1 in mouse induced pluripotent stem cells. *Nature*, **465** : 175-181, 2010.
20) Kim, K. et al. : Epigenetic memory in induced pluripotent stem cells. *Nature*, **467** : 285-290, 2010.
21) Polo, J. M. et al. : Cell type of origin influences the molecular and functional properties of mouse induced pluripotent stem cells. *Nat. Biotechnol.*, **28** : 848-855, 2010.

* * *

Development 139, 667-677 (2012) doi:10.1242/dev.072272

Genetic ablation of *Rest* leads to in vitro-specific derepression of neuronal genes during neurogenesis

Hitomi Aoki[1], Akira Hara[2], Takumi Era[3], Takahiro Kunisada[1] and Yasuhiro Yamada[4,5,*]

SUMMARY

Rest (RE1-silencing transcription factor, also called Nrsf) is involved in the maintenance of the undifferentiated state of neuronal stem/progenitor cells in vitro by preventing precocious expression of neuronal genes. However, the function of *Rest* during neurogenesis in vivo remains to be elucidated because of the early embryonic lethal phenotype of conventional *Rest* knockout mice. In the present study, we have generated *Rest* conditional knockout mice, which allow the effect of genetic ablation of *Rest* during embryonic neurogenesis to be examined in vivo. We show that *Rest* plays a role in suppressing the expression of neuronal genes in cultured neuronal cells in vitro, as well as in non-neuronal cells outside of the central nervous system, but that it is dispensable for embryonic neurogenesis in vivo. Our findings highlight the significance of extrinsic signals for the proper intrinsic regulation of neuronal gene expression levels in the specification of cell fate during embryonic neurogenesis in vivo.

KEY WORDS: Rest (Nrsf), Mouse model, Neurogenesis

INTRODUCTION

The establishment and maintenance of neuronal identity underlie the core of neuronal development. The transcriptional repressor RE1-silencing transcription factor [Rest; also known as neuron-restrictive silencer factor (Nrsf)], was initially discovered as a negative regulator of neuron-specific genes in non-neuronal cells (Chong et al., 1995; Schoenherr and Anderson, 1995). Rest is expressed throughout early development, where it represses the expression of neuronal genes and is involved in the transcriptional silencing of neuronal promoters in conjunction with CoRest (Rcor1/2) (Ballas et al., 2001), which recruits additional silencing machinery, including the methyl DNA-binding protein MeCP2, histone deacetylase (HDAC) and the histone H3K9 methyltransferase G9a (Ehmt2) (Andres et al., 1999; Lunyak et al., 2002; Roopra et al., 2004; Shi et al., 2003; You et al., 2001). Rest targets include a number of genes encoding ion channels, neurotrophins, synaptic vesicle proteins and neurotransmitter receptors (Bruce et al., 2004; Johnson et al., 2006; Otto et al., 2007). Indeed, a targeted mutation of *Rest* in mice caused derepression of neuron-specific tubulin in a subset of non-neuronal tissues, leading to embryonic lethality (Chen et al., 1998).

Mosaic inhibition of *Rest* in chicken embryos using a dominant-negative form of *Rest* also caused derepression of neuronal tubulin, as well as several other neuronal target genes, not only in non-neuronal tissues but also neuronal progenitors (Chen et al., 1998). These results suggest that *Rest* is required to repress the expression of neuronal genes in undifferentiated neuronal tissue. Expression of Rest is highest in embryonic stem cells (ESCs) and is downregulated as ESCs differentiate into neuronal stem cells (NSCs), and it is completely silenced in mature adult neuronal cells (Ballas et al., 2005). Given the fact that Rest represses the expression of a large number of neuronal genes, it is reasonable to expect that it plays a central role in the inhibition of the precocious expression of neuronal genes in NSCs, and that its downregulation upon receipt of neuronal differentiation cues permits the robust expression of differentiation-related neuronal genes, resulting in terminal differentiation (Ballas et al., 2005).

In addition to the involvement of Rest in neurogenesis, recent studies have demonstrated that Rest modulates glial lineage elaboration (Abrajano et al., 2009; Kohyama et al., 2010), suggesting that it also mediates the coupling of neurogenesis and gliogenesis, which might contribute to the neuronal-glial interactions that are associated with synaptic and neuronal network plasticity and homeostasis in the brain. Despite the expectation of a fundamental role of Rest in brain development, the function of Rest in NSCs and neuronal progenitors in the brain in vivo remains to be elucidated. *Rest* null mice survive to embryonic day (E) 9 without obvious morphological defects, by which time all three germ layers and the neural tube have formed, clearly demonstrating that neuronal progenitors can develop in vivo in the absence of *Rest* (Chen et al., 1998). However, *Rest* null mice die by E11.5 accompanied by gross morphological changes starting ~E9.5. This early embryonic lethality has precluded further analysis of the role of *Rest* in the maintenance and differentiation of NSCs and neural progenitor cells (NPCs) in vivo.

In addition to the possible role of *Rest* in neuronal/glial development, recent studies have indicated that the breakdown of these processes accompanies and promotes neurodegenerative disorders. The disruption of the interaction of Rest with its target genes was reported in epileptic seizures (Bassuk et al., 2008), Huntington's disease (Zuccato et al., 2007) and Down's syndrome (Canzonetta et al., 2008; Lepagnol-Bestel et al., 2009). In these disorders, Rest dysfunction is suggested to be a cause of aberrant changes in neuronal gene expression. Considering that abnormal expression of Rest has been seen in a variety of neurological and neurodegenerative diseases, it is important to uncover the

[1]Department of Tissue and Organ Development and [2]Department of Tumor Pathology, Regeneration, and Advanced Medical Science, Gifu University Graduate School of Medicine, Gifu, 501-1194, Japan. [3]Division of Molecular Neurobiology, Institute of Molecular Embryology and Genetics, Kumamoto University, Kumamoto 860-0811, Japan. [4]PRESTO, Japan Science and Technology Agency, 4-1-8 Honcho Kawaguchi, Saitama, Japan. [5]Center for iPS Cell Research and Application (CiRA), Institute for Integrated Cell-Material Sciences (iCeMS), Kyoto University, Kyoto 606-8507, Japan.

*Author for correspondence (y-yamada@cira.kyoto-u.ac.jp)

Accepted 18 December 2011

mechanisms that underlie how Rest suppresses the expression of neuronal genes to control neurogenesis and gliogenesis, and to provide a better understanding of the pathogenesis of such diseases.

In the present study, we have generated *Rest* conditional knockout mice that allow the effects of genetic ablation of *Rest* on brain development to be examined in vivo. We also examined the effect of *Rest* ablation in cells outside of the nervous system at different developmental stages.

MATERIALS AND METHODS

Animals

All animal experiments were approved by the Animal Research Committee of the Gifu University Graduate School of Medicine. $Rest^{2lox/2lox}$ mice were generated from the $Rest^{2lox/+}$ ESC line as described preciously (Yamada et al., 2010). *Rosa26::rtTA*; *Col1a1::tetO-Cre* mice (Yamada et al., 2010) and *Sox1-Cre/+* mice (Takashima et al., 2007) were bred with $Rest^{2lox/2lox}$ mice to generate compound transgenic mice. In order to induce Cre recombinase, doxycycline (2 mg/ml) was administered in the drinking water of the mice, supplemented with 10 mg/ml sucrose (Hochedlinger et al., 2005). To induce Cre-*loxP* recombination in the embryos, pregnant female mice were treated with doxycycline in their drinking water for 5 days, and were sacrificed on the last day of the doxycycline administration. In order to label neuronal stem/progenitor cells in the adult brain, BrdU was administered as a daily intraperitoneal injection of 50 mg/kg body weight for 12 days starting at the age of 8 weeks. The brains were fixed 1 day after the last injection (Shi et al., 2004).

Cell culture

For the neurosphere culture, brains were collected and dissociated into single-cell suspensions by gentle pipetting. The inner part of the trunk region was collected for genotyping. The primary neurospheres were formed from 1×10^5 suspended brain cells/well in a 24-well plate. The cells were cultured in DMEM/F12 supplemented with 1× N2 (Invitrogen), 1× B27 (Invitrogen), 20 ng/ml epidermal growth factor (EGF) (R&D Systems) and 20 ng/ml basic fibroblast growth factor (bFGF, or FGF2) (R&D Systems). The primary neurospheres were passaged to generate secondary neurospheres, which were used to compare neurosphere formation ability. For the adherent cultures of neurospheres, the spheres were inoculated into 6-well plates previously coated with fibronectin/laminin (both from Invitrogen) and cultured in DMEM/F12 supplemented with 1× B27 and 10% fetal calf serum (FCS) (Nichirei Bioscience, Tokyo, Japan).

MEFs were derived from small pieces of the outer part of the trunk region prepared as described above. The cells were seeded in 100-mm dishes and cultured in DMEM supplemented with 10% FCS. In order to induce *Rest* recombination in vitro, cultured cells were treated with doxycycline at 2 μg/ml. The cells were analyzed for GFP signals using a FACS Aria dual-laser flow cytometer (Becton-Dickinson).

Histology and immunohistochemistry

The brains were enucleated and fixed by immersion overnight in 10% formalin in phosphate buffer (pH 7.2). Specimens were dehydrated with ethanol, soaked in xylene and embedded in paraffin. Horizontal serial sections were prepared at 3μm using a Leica RM2125RT microtome and stained with Hematoxylin and Eosin (HE).

For immunohistochemistry, we used a Mouse-to-Mouse HRP Ready-To-Use Kit (ScyTek Laboratories) according to the manufacturer's protocol to detect the mouse monoclonal primary antibodies on the sections. For detection of the goat or rabbit polyclonal primary antibodies, a Histofine Kit (Nichirei Bioscience, Tokyo, Japan) or VECTASTAIN ABC Kit (Vector Laboratories) was used according to the manufacturers' protocol. Finally, the sections were stained with 3,3′-diaminobenzidine (DAB). For immunocytochemistry studies, cells were fixed with 4% PFA, made permeable by immersion in 0.1% Triton X-100, washed in PBS and blocked in 0.5% BSA. Primary antibodies were then added and allowed to react for 60 minutes at room temperature. After washing in PBS, the cells were stained with secondary antibodies. Cells were examined using an Olympus IX-71 fluorescence microscope.

Antibodies

The primary antibodies used in this study were: anti-mouse neuronal class III beta-tubulin (Tuj1; 1:5000; BabCO); anti-mouse glial fibrillary acidic protein (Gfap; 1:1000; Dako-Cytomation, Glostrup, Denmark); anti-human nestin (1:500; IBL, Gunma, Japan); anti-mouse nestin (1:1000; Chemicon); anti-mouse NeuN (1:1000; Chemicon); anti-BrdU (1:500; Dako-Cytomation); anti-doublecortin (Dcx; 1:500; Santa Cruz); anti-Prox1 (1:5000; Millipore); anti-radial glial cell marker 2 (clone RC2; 1:300; Millipore); anti-trimethyl histone H3 (Lys27) (1:200; Monoclonal Institute, Hokkaido, Japan).

Gene expression analysis

Total RNA was prepared using the RNeasy Plus Mini Kit (Qiagen) according to the manufacturer's instructions. The first-strand cDNA was synthesized from 1 μg total RNA using the SuperScript First-Strand Synthesis System (Takara, Shiga, Japan) with oligo(dT) primers. Real-time PCR was performed with SYBR Premix EX Taq (Takara) using Thermal Cycler Dice (Takara) for each gene of interest, and a β-actin endogenous control primer set was used for normalization. The primer sequences used in qRT-PCR analyses were obtained from PrimerBank (http://pga.mgh.harvard.edu/primerbank/).

The microarray analysis was performed according to the manufacturer's instructions (materials from Agilent unless otherwise stated). Briefly, cyanine-3 (Cy3)-labeled cRNA was prepared from 100 ng RNA using the One-Color Low RNA Input Liner Amplification Kit, followed by RNeasy column purification (Qiagen). Dye incorporation and cRNA yield were checked with a NanoDrop ND-1000 spectrophotometer. A total of 1.5 μg of Cy3-labeled cRNA (specific activity >10.0 pmol Cy3/μg cRNA) was fragmented at 60°C for 30 minutes in a reaction volume of 50 μl containing 1× fragmentation buffer and 2× blocking agent following the manufacturer's instructions. On completion of the fragmentation reaction, 50 μl 2× HI-RPM Hybridization Buffer was added and hybridized to Whole Mouse Genome Oligo Microarrays (G4122F) for 17 hours at 65°C in a rotating hybridization oven. After hybridization, microarrays were washed for 1 minute at room temperature with GE Wash Buffer 1 and 1 minute at 37°C with GE Wash buffer 2, then dried immediately by brief centrifugation. Slides were scanned immediately after washing on a DNA microarray scanner (G2565B) using the one-color scan setting for 4×44k array slides [scan area 75×25 mm, scan resolution 5 μm, dye channel set to green and green PMT set to 10-100% (XDR)]. The scanned images were analyzed with the Feature Extraction Software package v. 9.5.3.1 using default parameters (protocol GE1-v5_95_Feb07 and Grid: 014868_D_F_20101102) to obtain background-subtracted and spatially detrended processed signal intensities. Data were analyzed using GeneSpring software.

RESULTS

Conditional ablation of the CoRest binding site in developing embryos results in embryonic lethality

In order to examine the effect of *Rest* deletion in vivo, we generated mice containing floxed *Rest* alleles and doxycycline-inducible *Cre* alleles ($Rest^{2lox/2lox}$; *Rosa26::rtTA*; *Col1a1::tetO-Cre*), in which exon 4, which encodes the CoRest binding site, can be removed upon treatment of mice with doxycycline (Fig. 1A) (Andres et al., 1999; Beard et al., 2006; Fink et al., 1999; Hatano et al., 2011; Yamada et al., 2010). Rest contains two repressor domains (Tapia-Ramirez et al., 1997): an N-terminal domain that associates with HDACs and Sin3; and a C-terminal domain that interacts with CoRest (Andres et al., 1999). Importantly, although our recombined *Rest* knockout (KO) allele ($Rest^{1lox}$) still contains exons 1-3, which encode the N-terminal domain of Rest, altered *Rest* transcript was not detected in our $Rest^{1lox/1lox}$ mouse ESCs, suggesting that the $Rest^{1lox}$ allele in this system is equivalent to the conventional KO allele (Yamada et al., 2010). We further demonstrated that *Stmn2* (*SCG10*), a CoRest-independent target of Rest-mediated repression (Jepsen et al., 2000; Lunyak et al., 2002),

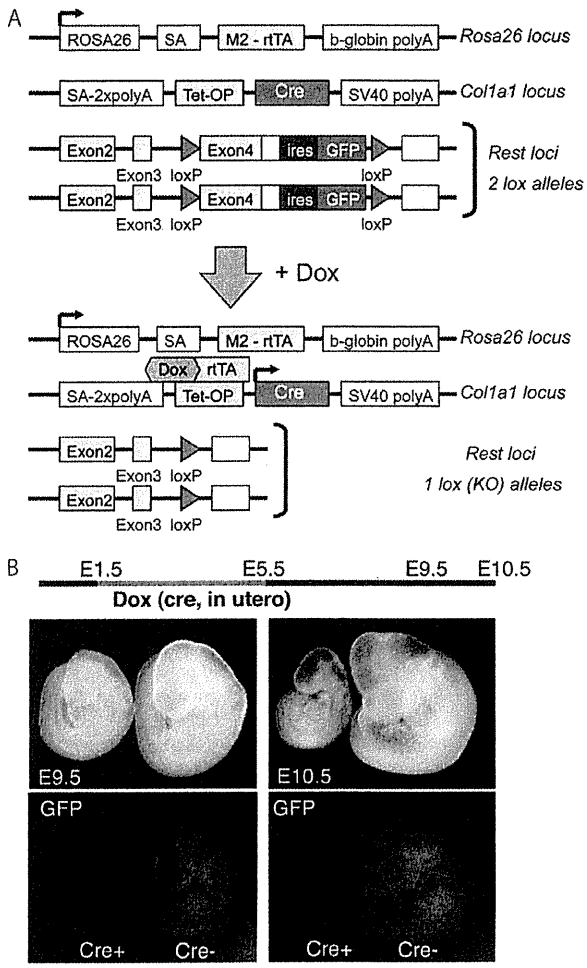

Fig. 1. Conditional *Rest* knockout mice. (**A**) In the conditional *Rest* knockout (KO) mice, exon 4 of *Rest* can be removed by doxycycline (Dox) exposure. (**B**) Pregnant mice with *Rest* conditional KO embryos were treated with doxycycline to delete the *Rest* alleles from the embryos in utero (E1.5-5.5). The growth retardation phenotype is detectable at E9.5 and E10.5.

is upregulated in $Rest^{1lox/1lox}$ mouse ESCs (supplementary material Fig. S1), indicating again that our *Rest* KO cells are equivalent to the *Rest* null cells.

A previous study using conventional KO mice revealed that mice lacking the *Rest* gene die during early embryonic development (Chen et al., 1998). When we administrated doxycycline to the *Rest* conditional KO embryos to delete the *Rest* gene in utero (E1.5-5.5), we observed lethality of the embryos carrying the *tetO-Cre* allele at ~E10.5 with a growth retardation phenotype, which was accompanied by the loss of GFP signals, indicating that the phenotype of the conventional KO mice could be recapitulated in our *Rest* conditional KO mice (Fig. 1B).

Genetic ablation of *Rest* in non-neuronal cells outside of the central nervous system in vitro

Previous studies suggest that *Rest* is expressed in a variety of non-neuronal cells to suppress the neuronal differentiation of these cells. Indeed, the conventional *Rest* KO mice showed ectopic expression of Rest target genes, such as *Tuj1* (*Tubb3*), in non-neuronal cells outside of the brain (Chen et al., 1998). Therefore, to elucidate whether *Rest* ablation can induce the expression of Rest target genes in non-neuronal cells, we used mouse embryonic fibroblasts (MEFs) containing floxed *Rest* alleles and doxycycline-inducible *Cre* alleles ($Rest^{2lox/2lox}$; *Rosa26*::*rtTA*; *Col1a1*::*tetO-Cre*). The *Rest* conditional KO MEFs were treated with doxycycline for 3 days starting 1 day after the seeding of the MEFs (passage 1). Seven days after the seeding of the MEFs, the MEFs were examined for GFP expression by FACS analysis. Three weeks after the seeding of the MEFs, they were analyzed by immunocytochemistry with a Tuj1 antibody to detect expression of the neural cell marker. The expression of Rest target genes was also examined by real-time RT-PCR 3 weeks after the seeding of the MEFs.

Consistent with the recombination, FACS analysis revealed a decreased GFP signal in the *Rest* conditional KO MEFs treated with doxycycline (Fig. 2A). As demonstrated in a previous study using conventional KO mice, deletion of *Rest* caused an increase in the expression of Tuj1 in MEFs (Fig. 2B) (Chen et al., 1998). The real-time RT-PCR revealed that MEFs treated with doxycycline expressed a significantly reduced level of *GFP* and *Rest* (Fig. 2C). We found that this was associated with increased expression of *Syt4*, *Tubb3* and *Calb1*, which contain RE1 sites and are targets of the Rest repressor complex (Chong et al., 1995; Johnson et al., 2008; Schoenherr and Anderson, 1995; Schoenherr et al., 1996) (Fig. 2C). We also found that *Stmn2*, a CoRest-independent target of Rest-mediated repression, was also derepressed in MEFs by doxycycline exposure (Fig. 2C). These results indicate that Rest target genes are rapidly derepressed upon the loss of *Rest* in MEFs. However, *Bdnf*, which also contains an RE1 site and is a target of the Rest repressor complex in ESCs/NSCs (Johnson et al., 2008; Yamada et al., 2010), did not show any detectable derepression in doxycycline-treated MEFs (Fig. 2C).

Although we confirmed that removal of the *Rest* CoRest binding site induces ectopic neuronal gene expression in non-neuronal cells outside of the brain, it remains unclear whether *Rest* ablation can actually induce neuronal differentiation in non-neuronal cells. In the present study, despite the observed increase in the expression of neuronal genes such as *Syt4*, *Tubb3*, *Calb1* and *Stmn2* after ablation of *Rest* in MEFs, the morphology of the Tuj1-expressing cells did not change (Fig. 2B). In addition, the expression of *Fsp1* (*S100a4*), a marker for fibroblasts (Strutz et al., 1995), was not decreased in the Tuj1-expressing MEFs (supplementary material Fig. S2). These findings suggest that *Rest* ablation in non-neuronal cells leads to ectopic neuronal gene expression, but that its ablation is not sufficient to induce transdifferentiation into neuronal cells (Vierbuchen et al., 2010).

We also examined the effect of *Rest* ablation in adult non-neuronal cells in vitro using tail tip fibroblasts (TTFs) containing the floxed *Rest* alleles and doxycycline-inducible *Cre* alleles. After exposure to doxycycline, we detected significant upregulation of the Rest target genes *Syt4*, *Tubb3*, *Calb1* and *Stmn2* in the TTFs, which was accompanied by the downregulation of *Rest* and *GFP* expression (supplementary material Fig. S3). Consistent with the results in MEFs, we failed to detect derepression of *Bdnf* or downregulation of *Fsp1* in TTFs after *Rest* ablation (supplementary material Fig. S3). We also conditionally deleted the *Rest* CoRest binding site in adult mice by the administration of doxycycline in the drinking water, and examined the expression of Rest target genes in the tail tissues. We confirmed the derepression of Rest target genes in the adult tail tissues after genetic ablation of *Rest* in vivo (supplementary material Fig. S4).